






Article

Pain-Related White-Matter Changes Following Mild Traumatic Brain Injury: A Longitudinal Diffusion Tensor Imaging Pilot Study

Ho-Ching Yang ¹, Tyler Nguyen ^{2,3}, Fletcher A. White ^{2,3,†}, Kelly M. Naugle ^{4,†} and Yu-Chien Wu ^{1,3,5,*,†}

¹ Department of Radiology and Imaging Sciences, Indiana University School of Medicine, Indianapolis, IN 46202, USA

² Department of Anesthesia, Indiana University School of Medicine, Indianapolis, IN 46202, USA

³ Stark Neurosciences Research Institute, Indiana University School of Medicine, Indianapolis, IN 46202, USA

⁴ Department of Kinesiology, School of Health and Human Sciences, Indiana University Indianapolis, Indianapolis, IN 46202, USA

⁵ Weldon School of Biomedical Engineering, Purdue University, West Lafayette, IN 47906, USA

* Correspondence: yucwu@iu.edu; Tel.: +1-317-963-1697

† Senior authors.

Abstract: Background: This study used diffusion tensor imaging (DTI) to detect brain microstructural changes in participants with mild traumatic brain injury (mTBI) who experienced post-traumatic headaches, a common issue that affects quality of life and rehabilitation. Despite its prevalence, the mechanisms behind post-traumatic headache are not well understood. **Methods:** Participants were recruited from Level 1 trauma centers, and MRI scans, including T1-weighted anatomical imaging and DTI, were acquired 1 month post-injury. Advanced imaging techniques corrected artifacts and extracted diffusion tensor measures reflecting white-matter integrity. Pain sensitivity assays were collected at 1 and 6 months post-injury, including quantitative sensory testing and psychological assessments. **Results:** Significant aberrations in axial diffusivity in the forceps major were observed in mTBI participants ($n = 12$) compared to healthy controls ($n = 10$) 1 month post-injury ($p = 0.02$). Within the mTBI group, DTI metrics at 1 month were significantly associated with pain-related and psychological outcomes at 6 months. Statistical models revealed group differences in the right sagittal stratum ($p < 0.01$), left insula ($p < 0.04$), and left superior longitudinal fasciculus ($p < 0.05$). **Conclusions:** This study shows that DTI metrics at 1 month post-injury are sensitive to mTBI and predictive of chronic pain and psychological outcomes at 6 months.



Academic Editor: Hidehiko Okazawa

Received: 19 January 2025

Revised: 28 February 2025

Accepted: 3 March 2025

Published: 6 March 2025

Citation: Yang, H.-C.; Nguyen, T.; White, F.A.; Naugle, K.M.; Wu, Y.-C. Pain-Related White-Matter Changes Following Mild Traumatic Brain Injury: A Longitudinal Diffusion Tensor Imaging Pilot Study.

Diagnostics **2025**, *15*, 642.

<https://doi.org/10.3390/diagnostics15050642>

Copyright: © 2025 by the authors. Licensee MDPI, Basel, Switzerland. This article is an open access article distributed under the terms and conditions of the Creative Commons Attribution (CC BY) license (<https://creativecommons.org/licenses/by/4.0/>).

Keywords: mild traumatic brain injury; diffusion tensor imaging; post-traumatic headache; endogenous pain measure; psychological-related assessments

1. Introduction

Post-traumatic headache (PTH) is a significant and enduring consequence of mild traumatic brain injury (mTBI), with a prevalence ranging from 30% to 90% in civilian adult populations [1–3]. It is defined as a secondary headache that develops within 7 days following the injury [4]. PTH is regarded as chronic when it continues for more than 3 months, with 18–22% lasting more than 1 year [5,6] and approximately 2–5% lifetime prevalence [7]. Therefore, effective intervention and treatment will benefit millions of affected individuals, if the underlying PTH pathogenesis can be clarified by identifying reliable biomarkers.

Considerable overlap exists between PTH and more common headache disorders, such as migraine. However, migraine-specific preventive medications are largely reported to be ineffective for PTH [8]. PTH mechanisms responsible for pathophysiology likely include abnormal endogenous pain modulation, activation of the somatosensory system, and psychological symptoms. Previous studies have demonstrated that mTBI produces sensitization of the head area (i.e., lower pressure pain thresholds (PPT) in the head region) and reduced pain inhibition during the conditioned pain modulation (CPM) test when compared to healthy controls [9]. Reduced pain-inhibitory capacity, soon after the injury, is a risk factor for the development of persistent PTH [9]. These results have been mirrored in pre-clinical studies demonstrating impaired descending noxious inhibitory controls and heightened sensitization to noxious mechanical stimuli in mice for a duration of up to 2 weeks after mTBI [10]. Further, multiple studies have reported increased anxiety, depression, and pain catastrophizing among patients with persistent PTH [9,11].

Diffuse axonal injury is also generally believed to be the initial neuropathology associated with mTBI [12–14]. A few studies report evidence of diffuse axonal injury in post-mortem pathological examination of human mTBI. These papers suggest severing of nerve fibers without hemorrhage [15], the presence of amyloid precursor protein indicating axonal damage [16], and polarized macrophages in white matter [17]. Additionally, evidence of axonal injury in conjunction with chronic traumatic encephalopathy has been demonstrated in football players exposed to repetitive head impacts and/or concussion [18].

Nevertheless, this microscopic white-matter injury has been more difficult to detect in human mTBI with in vivo approaches. Neuroimaging may provide significant advancement for quantitatively detecting and characterizing the mechanisms of brain changes associated with pain-related outcomes following mTBI. While conventional diagnostic magnetic resonance imaging (MRI) presents negative findings in PTH after mTBI, recent studies have explored advanced imaging modalities to provide better diagnostic and prognostic utility [19,20]. For example, functional MRI has been widely used to explore both ascending and descending nociceptive pathways in the cortico-mesolimbic system for patients with chronic pain [21–25]. Also, susceptibility-weighted imaging (SWI) is capable of detecting localized microbleeds that are highly associated with axonal injury in mTBI [26,27], but it has not been used for PTH detection. Furthermore, arterial spin labeling has been used to assess cerebral perfusion impairment in mTBI. Despite inconsistent results, more findings indicate decreased rather than increased cerebral blood flow after mTBI [28,29]. With respect to PTH, perfusion-based functional connectivity of the insular subregion has been shown to be significantly associated with headache features [30], but interestingly, it did not show significant associations in female PTH at 2 weeks after pediatric concussion [31].

Diffusion MRI, however, may offer greater sensitivity in comparison with the imaging modalities mentioned above for detecting white-matter microstructure changes in mTBI [32–34]. The classic diffusion tensor imaging (DTI) has been widely used in white-matter diseases and was found to have adequate diagnostic sensitivity to microstructural changes in the brain after mTBI [35–44]. Despite its popularity, there have been few DTI studies focusing on PTH. In these few studies, scientists have observed white-matter differences between participants with and without PTH [45–47]. For example, patients with mTBI and PTH exhibited lower fractional anisotropy (FA) in the corpus callosum and fornix/septohippocampal circuit in comparison with healthy controls [48]. Similar findings of lower FA were found in the genu of the corpus callosum in mTBI patients with PTH compared to healthy controls by utilizing a principal component analysis [49]. A recent study investigated the association between white-matter structural connectivity and quantitative pain measurements but without providing further characteristics of white-matter microstructure [50]. While these studies provide insights into one DTI metric (i.e., FA) in

PTH, they did not leverage the full potential of DTI by including all four metrics to encompass a holistic interpretation for microstructural changes in white matter in PTH. Moreover, previous studies (except [49]) did not include pain-related outcomes in the analyses. To address these knowledge gaps, this study will investigate all four DTI metrics, including FA, mean diffusivity (MD), radial diffusivity (RD), and axial diffusivity (AD), with a comprehensive survey of pain-related outcomes, including quantitative, psychological, and clinical pain assessments.

In this pilot study, we characterized white-matter microstructural alterations in mTBI patients with headache or at risk of developing headache. We studied (1) between-group differences (mTBI and control) at 1 month post-injury, (2) associations between early DTI metrics at 1 month post-injury and later pain- and psychological-related assessments at 6-month post-injury to examine the predictivity of DTI metrics in mTBI group, and (3) between-group (mTBI and control) prediction power differences for those significant associations within mTBI group.

2. Materials and Methods

2.1. Participants

The clinical coordinators screened electronic patient medical records for patients who had experienced mTBI and also met the associated inclusion and exclusion criteria. The mTBI diagnosis for each patient is outlined by the World Health Organization Task Force [51]. Next, potentially qualified mTBI patients' identification and contact information were entered into a secure database for recruitment. Age- and sex-matched control participants with no TBI history were also recruited from the community, following the same exclusion criteria as outline below [52].

The inclusion criteria for the mTBI participants were level of consciousness, a clean CT test, experience of an altered mental status, and an adult under the age of 66. Secondly, the exclusion criteria included cardiovascular disorders, chronic systemic diseases, neurologic disorder, severe mental health disorder, previous chronic migraine, active legal proceedings, prolonged narcotic dependence, head injuries with fractural trauma, metallic implants, cognitive impairment, or pregnancy [52].

All mTBI participants received pain and psychological assessments at 1 month and 6 months post-injury [52]. A subset of the mTBI participants ($n = 13$) received MRI scans at 1 month post-injury and was included in this study to investigate the relationship and predictivity of neuroimaging and later pain-related outcomes. The controls ($n = 10$) completed two study sessions separated by 5–6 months and received the same pain and psychological assessments and neuroimaging.

2.2. Quantitative Pain Assessments

Quantitative sensory tests (QSTs) were used to measure pain sensitivity of the head and endogenous pain modulation. These tests included temporal summation of pain (TS) as an indirect method of assessing hyperexcitability of the central nervous system [53], PPTs measuring trigeminal sensitization [54], and conditioned pain modulation (CPM) assessing endogenous pain inhibition [55,56]. The TS test was performed first, followed by PPTs of the head, and then the CPM test. Before each session, all participants were asked to refrain from pain-relief medication and consuming caffeine on the day of testing.

Mechanical Temporal Summation (TS) was tested on the middle of the forehead and the back of the hand using a Von Frey filament (Touch test Sensory Evaluator 6.65, North Coast Medical, Inc., Morgan Hill, CA, USA) calibrated to bend at 300 g of pressure. First, a single pinprick with the filament was applied to the body site. Then, a series of 10 pinpricks with the same filament was applied to the same body site within an area of 1 cm² and at a rate

of 1 prick per second. Participants rated their pain after the single pinprick and after the series of 10 pinpricks using a 0–100 scale. TS was calculated as the difference between the single-pinprick pain-rating and the series of 10-pinpricks pain-rating. This TS procedure was administered twice with pauses at each location, then averaged for one forehead and hand scores [52].

Pressure Pain Thresholds of the Head (PPTs) were assessed by measuring sensory response on the head with an algometer. The probe was applied in two series, separated by a pause, with constant pressure against the skin on five sites. Participants alerted the examiner when first experiencing pain during the test. The scores from all trials were averaged to obtain one score for each participant [52].

Conditioned Pain Modulation (CPM) evaluates whether pain produced by a test stimulus is diminished by a second painful conditioning stimulus applied to a remote body site [55,56]. In this study, one hand was submerged in a cold-water bath (conditioning stimuli), and the PPTs (test stimuli) were immediately conducted on the opposite arm. This sequence was repeated for a second time. The magnitude of CPM reveals the amount of the altered-pain threshold following conditional stimuli [52].

2.3. Psychological and Clinical Pain Assessments

Head pain and psychological measures were collected via validated questionnaires as described below.

Headache survey: The participant survey was designed to demonstrate the severity of headache intensity (HA), including a range of related factors. Headache intensity was used for data analysis [52].

McGill Pain Questionnaire (MPQ) offers an objective level and description of the pain a participant is experiencing [57]. The pain-rating index (PRI) provides a descriptive ranking for the severity of a person's associated pain.

Defense and Veterans Pain Rating Scale (DVPRS): 0 indicates “no pain”, and 10 indicates “as bad as it could be, nothing else matters” [58].

TBI Quality of Life (TBI-QOL) Headache Form assesses the severity and impact of headaches over the last 7 days with 10 items [59].

Post-Traumatic Stress Disorder (PTSD) for DSM-5 (PCL-5) is a 20-item scale that is designed to evaluate the DSM-5 symptoms of PTSD, and it is used for diagnosis and as a severity measure [60].

Pain-Catastrophizing Scale (PCS) uses the Likert scale to assess a participant's mental condition, demonstrating the effect of negative thoughts resulting in actual pain. Higher scores indicate greater pain catastrophizing [61].

Center for Epidemiological Studies—Depression Scale (CES-D) is a self-report depression scale used to evaluate participant symptoms [62].

2.4. Image Acquisition

The participants underwent MRI scans in Siemens MAGNETOM Biography mMR 3T scanner (Siemens Medical Solutions USA, Inc., Malvern, PA, USA) with a 20-channel head/neck coil. The MRI scans included T1-weighted anatomical imaging and diffusion-weighted imaging (DWI). The total MRI examination time is 44 min and 38 s. The T1-weighted images were acquired by inversion recovery-prepared spoiled gradient-echo (IRSPGR) with TR/TE = 1960/2.19 ms, flip angle = 10 deg, and $1.0 \times 1.0 \times 1.0 \text{ mm}^3$ voxels, with a scan time of 4 min and 34 s. Diffusion MRI was performed with a single-shot echo-planar imaging sequence and consisted of 64 directions at b value of 1000 s/mm^2 and 1 b0 (b value = 0 s/mm^2). Other imaging parameters were field-of-view = 2080 mm, 60 slices, voxel size = $2.0 \times 2.0 \times 2.0 \text{ mm}^3$, TR/TE = 10,900/79 ms, in-plane GRAPPA

acceleration factor = 2, with a scan time of 12 min and 21 s. For distortion correction, a dual-echo gradient-echo sequence (GRE) was used to acquire the field map with TR = 400 ms, TE = 4.92/7.38 ms, with a scan time of 54 s.

2.5. Diffusion MRI Data Analysis

The DWI were initially denoised with a Marchenko–Pastur principal component analysis approach [63] followed by Gibbs ringing artifacts removal using local subvoxel-shifts command in MRtrix3 (mrdegibbs; www.mrtrix.org) [64]. The motion, eddy current, and susceptibility artifacts correction were performed by using a dual-echo GRE field-map and T1-weighted image with the eddy_openmp command provided in the FMRIB Software Library (FSL; <https://fsl.fmrib.ox.ac.uk/fsl/docs/#/>) [65]. The FSL eddy command detects outlier slices using a Gaussian process prediction. B1 field inhomogeneity was also corrected (MRtrix3 dwibiascorrect) [66]. Four classic DTI metrics were calculated and registered to the Montreal Neurological Institute (MNI) template using a nonlinear registration tool, ANTs (Advanced Neuroimaging Tools) [67]. The DTI metrics included fractional anisotropy (FA), mean diffusivity (MD), radial diffusivity (RD), and axial diffusivity (AD).

A study-specific, whole-brain, white-matter skeleton was created using the FSL toolbox [68]. Eighteen bilateral regions-of-interest (ROIs) were segmented by intersecting the white-matter skeleton template and the JHU White-Matter Tractography Atlas [47,68,69] (Figure 1).

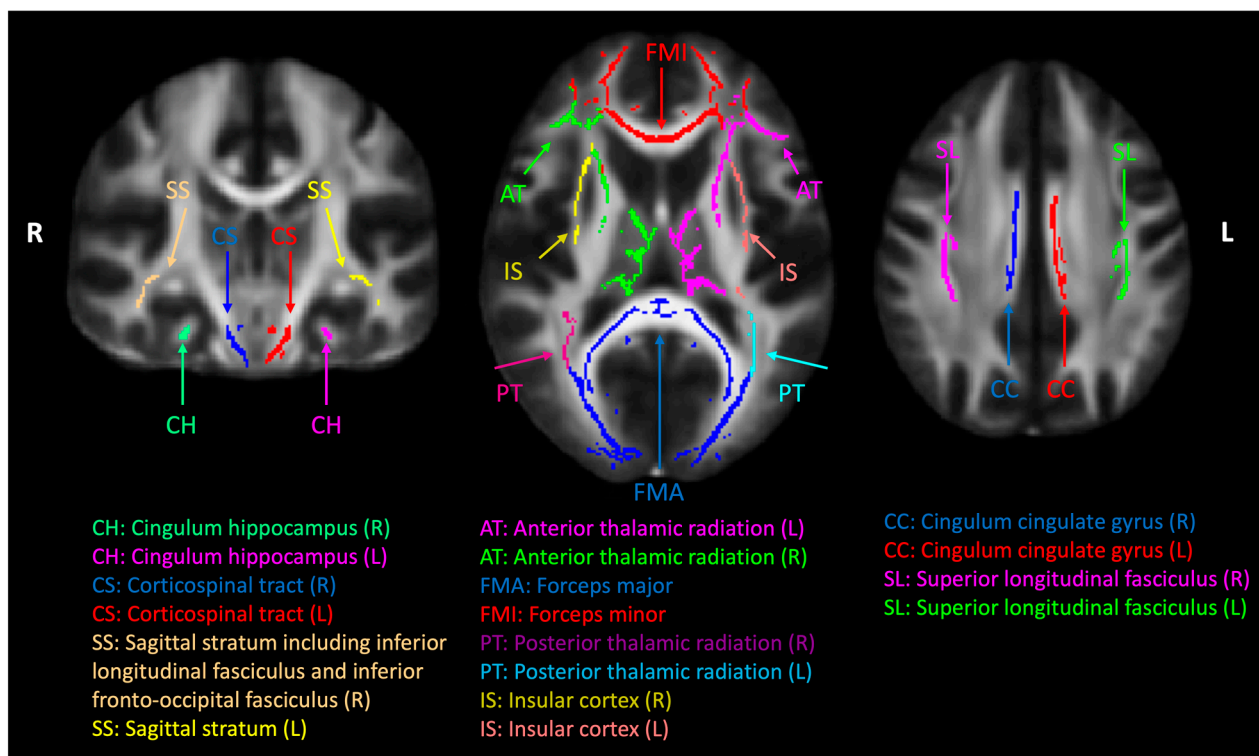


Figure 1. Cerebral white-matter tract regions of interest (ROIs). A common white-matter skeleton was first generated by the tract-based spatial statistics (TBSS) toolbox in the FMRIB Software Library (FSL) using normalized diffusion tensor imaging (DTI) fractional anisotropy maps from all the subjects. The white-matter skeleton was intersected with Johns Hopkins University (JHU) white-matter tract atlas, and eighteen ROIs were used in this study.

2.6. Statistical Analysis

The Kolmogorov–Smirnov test of normality indicated that most of the diffusion metrics, QSTs, psychological, and clinical measures followed a normal distribution in both groups (see Supplementary Tables S1 and S2 for details). However, normality was not observed in headache, MPQ, and TBIQL scores for the control group, as the majority of control participants had a score of 0 for headache ($n = 9$), MPQ ($n = 9$), and TBIQL ($n = 8$). In such cases, normality testing is not meaningful because a distribution with a large proportion of identical values (such as 0) is not continuous and will not follow a normal distribution. Thus, parametric tests were used to analyze these data. This study utilized a two-sample independent T-test to examine group differences in continuous variables related to demographic and clinical outcome measures, as presented in Table 1. Sex, as a categorical variable, was analyzed using χ^2 tests to assess differences in sex compositions across groups. Generalized linear regression models were used to test (1) group differences in the DTI metrics between mTBI and control participants at 1 month, (2) associations of the early DTI metrics at 1 month with later outcome measures at 6 months to assess predictivity of DTI in mTBI, and (3) group differences in the predictivity of DTI for pain and psychological outcome measures. For the group differences in the DTI metrics, we used Model 1 controlling for age and sex, as well as the DVPRS pain rating, to minimize the effect of acute general pain and to focus on chronic headache at the time of MRI scans (Equation (1)). For the predictivity evaluation in the mTBI group, we used Model 2 controlling for age, sex, and the DVPRS scores (Equation (2)). Since there is a possibility of observing similar significant associations in control participants as well as those significant associations in mTBI participants in Model 2, we further tested whether there were group (mTBI and control) differences in the predictivity of DTI using Model 3 (Equation (3)), which included an interaction term of “group*DTI”. Specifically, if β_3 in Model 3 was significant (i.e., $p_{\text{int}} < 0.05$), there would be significant group differences in the associations between outcomes_{6-mo} and DTI_{1-mo}. When the interaction term is significant (i.e., $p_{\text{int}} < 0.05$), we performed post hoc correlation analyses in the control group using Model 2 and compare the scatterplots between the 2 groups. The significance threshold was set at $p < 0.05$ for all tests, with exact p -values for each measure reported in the Results Section. Due to the exploratory nature of this pilot study and small sample size, we did not adjust for multiple comparisons [70].

Model 1:

$$DTI_{\text{metrics}} = \beta_0 + \beta_1 \cdot \text{group} + \beta_2 \cdot \text{age} + \beta_3 \cdot \text{sex} + \beta_4 \cdot \text{DVPRS} + \varepsilon \quad (1)$$

Model 2:

$$\text{Outcomes}_{6\text{mo}} = \beta_0 + \beta_1 \cdot \text{DTI}_{1\text{mo}} + \beta_2 \cdot \text{age} + \beta_3 \cdot \text{sex} + \beta_4 \cdot \text{DVPRS} + \varepsilon \quad (2)$$

Model 3:

$$\begin{aligned} \text{Outcomes}_{6\text{mo}} = & \beta_0 + \beta_1 \cdot \text{DTI}_{1\text{mo}} + \beta_2 \cdot \text{group} + \beta_3 \cdot \text{group} \cdot \text{DTI}_{1\text{mo}} + \beta_4 \cdot \text{age} \\ & + \beta_5 \cdot \text{sex} + \beta_6 \cdot \text{DVPRS} + \varepsilon \end{aligned} \quad (3)$$

Table 1. Demographic, pain, psychological, and clinical measurements of the participants.

| | Time Point | mTBI | Control | <i>p</i> -Value |
|----------------------------------|------------|-----------------|-----------------|-----------------|
| Demographics | | | | |
| Sample size (<i>n</i>) | | 12 | 10 | N/A |
| Age (year) | | 34.00 (8.09) | 31.30 (8.38) | 0.45 |
| Sex (male:female) | | 9:3 | 5:5 | 0.44 * |
| Quantitative sensory tests (QST) | | | | |
| TS | 1 mo | 12.13 (17.66) | 15.25 (16.97) | 0.68 |
| | 6 mo | 9.8 (18.48) | 12.22 (5.42) | 0.71 |
| PPT | 1 mo | 293.95 (149.38) | 344.61 (115.00) | 0.39 |
| | 6 mo | 333.82 (182.03) | 411.80 (115.37) | 0.29 |
| CPM | 1 mo | 13.27 (18.17) | 23.02 (18.90) | 0.23 |
| | 6 mo | 49.39 (91.00) | 21.26 (17.45) | 0.40 |
| Psychological measures | | | | |
| PCS | 1 mo | 13.17 (11.33) | 13.20 (11.55) | 0.99 |
| | 6 mo | 14.60 (10.32) | 23.11 (17.59) | 0.21 |
| PCL | 1 mo | 23.08 (18.74) | 8.10 (6.06) | 0.03 |
| | 6 mo | 24.00 (22.42) | 9.00 (9.25) | 0.08 |
| CES-D | 1 mo | 18.42 (13.10) | 8.30 (8.21) | 0.04 |
| | 6 mo | 16.90 (13.39) | 8.56 (8.32) | 0.13 |
| Clinical measures | | | | |
| HA | 1 mo | 6.00 (2.68) | 0.70 (2.21) | 0.0001 |
| | 6 mo | 5.11 (3.69) | 0.78 (2.33) | 0.01 |
| MPQ | 1 mo | 10.25 (6.05) | 0.10 (0.32) | 0.0001 |
| | 6 mo | 7.60 (5.50) | 1.22 (3.67) | 0.01 |
| TBI-QOL | 1 mo | 22.33 (5.65) | 1.00 (3.16) | 0.00001 |
| | 6 mo | 23.30 (13.05) | 2.33 (4.64) | 0.001 |
| DVRS pain rating at MRI scan | 1 mo | 3.17 (2.33) | 0.00 (0.00) | 0.001 |

Data are presented as mean (standard deviation) or male: female. Two tailed *t*-tests were used unless noted otherwise. Bold numbers indicate statistical significance with $p < 0.05$. * denotes Pearson's Chi-square tests used for sex.

3. Results

Thirteen mTBI and ten control participants received neuroimaging at 1 month post-injury. One mTBI participant's MRI data were excluded due to an extended artifact from a dental implant, making the final sample size for the mTBI group twelve. The demographic characteristics of the participants are listed in Table 1. There were no significant differences between the mTBI and control participants in age ($p = 0.45$) and sex ($p = 0.44$). Compared to the controls, the mTBI participants had significantly higher scores on the PCL ($p = 0.03$) and CES-D ($p = 0.04$) at 1 month post-injury and higher scores in all the clinical pain measures (i.e., HA, MPQ, TBIQL, and DVPRS) ($p < 0.01$) at 1 month and 6 months post-injury. Moreover, it is noteworthy that our mTBI participants exhibited significant headache symptoms. Eleven mTBI participants reported experiencing new or worse headaches within 1 week of the mTBI, which were still present at 1 month post-injury. Nine of these mTBI participants still reported experiencing regular headaches at 6 months post-injury

(data missing for 2 participants). The average headache-intensity score among the mTBI participants was significantly higher than the controls at 1 month post-injury ($p = 0.0001$) and at 6 months post-injury ($p = 0.01$).

Approximately half of the mTBI participants reported taking medications for their headaches. Specifically, at the 1 month post-injury visit, six participants reported taking medications for their headaches, including acetaminophen ($n = 4$), NSAIDS ($n = 6$), medicine that treats muscle spasms ($n = 1$), and anti-anxiety ($n = 1$) and antidepressant ($n = 1$) medicine. At the 6 months post-injury visit, seven participants reported taking medications for their headaches, including acetaminophen ($n = 4$), triptans ($n = 1$), NSAIDS ($n = 4$), and anti-anxiety ($n = 1$) and antidepressant ($n = 1$) medicine. All participants reported taking the medicine only when a headache was present (i.e., for abortive purposes). These medications were not taken on the day of testing, before the session took place.

Abbreviations: mild traumatic brain injury (mTBI); p = significance level; mo = month; TS = temporal summation of pain measuring endogenous facilitation of pain of the forehead areas; PPT = pressure pain threshold measuring sensitization of the head area; CPM = conditioned pain modulation measuring endogenous pain inhibition; PCS = pain catastrophizing scale; PCL = post-traumatic stress symptoms questionnaire; CES-D = Center for Epidemiological Studies—Depression scale; HA = headache intensity; MPQ = McGill Pain Questionnaire measuring different aspects of head pain in the past week; TBI-QOL = TBI Quality of Life Headache scale measuring subjective experience of headache symptoms for those with TBI; DVRS = Defense and Veterans Pain Rating Scale.; MRI = magnetic resonance imaging.

3.1. Group Differences in the DTI Metrics

The mTBI participants exhibited significantly lower AD in the forceps major ($p = 0.02$) than the controls at 1 month post-injury (Figure 2). Other DTI metrics and white-matter fiber tracts did not differ significantly between groups.

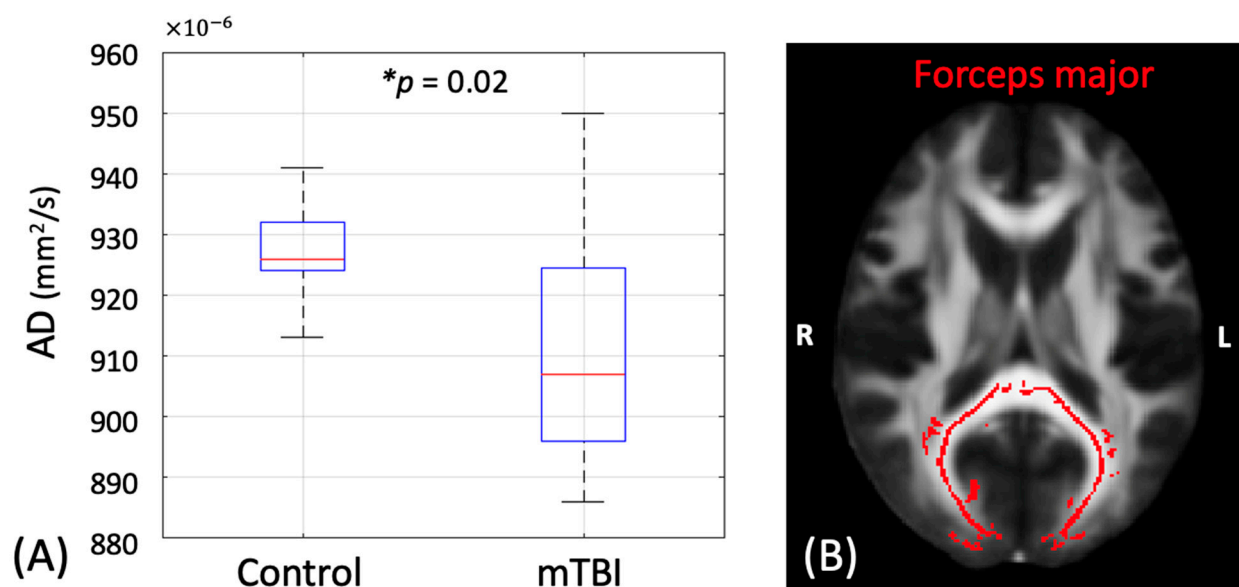


Figure 2. (A) Bar plot of DTI axial diffusivity (AD) between the mild traumatic brain injury (mTBI) participants and controls in the forceps major at 1 month post-injury. * denotes significant p value less than 0.05. (B) The forceps major fiber tract is highlighted in red. The image is presented in radiology orientation.

3.2. Association Between the Early DTI Metrics and Later Pain- and Psychological-Related Measures

Within the mTBI group, the DTI metrics at 1 month post-injury had significant associations with the pain-related measures at 6 months post-injury (Table 2). The QST TS of the head was predicted by DTI FA in the right sagittal stratum, including the inferior longitudinal fasciculus and inferior frontal occipital fasciculus, with a large correlation coefficient, $r = -0.60$ ($p = 0.01$). The QST PPT was predicted by DTI AD in the left anterior thalamic radiation, corticospinal tract, and insula with a moderate correlation coefficient, $r > 0.13$ ($p < 0.05$). Furthermore, CPM had a significant positive association with FA in left superior longitudinal fasciculus ($r = 0.83$, $p = 0.02$).

Table 2. Significant associations between the DTI metrics of the mTBI participants at 1 month post-injury and pain-related measures at 6 months post-injury.

| | DTI Metrics | <i>p</i> | <i>r</i> | <i>R</i> ² |
|---------------------------------------|-------------|----------|----------|-----------------------|
| Quantitative sensory tests (QST) | | | | |
| Right sagittal stratum | | | | |
| TS | FA | 0.01 | −0.60 | 0.80 |
| Left anterior thalamic radiation | | | | |
| PPT | AD | 0.04 | 0.23 | 0.87 |
| Left corticospinal tract | | | | |
| PPT | AD | 0.01 | 0.35 | 0.94 |
| Left insula | | | | |
| PPT | AD | 0.02 | 0.13 | 0.90 |
| Left superior longitudinal fasciculus | | | | |
| CPM | FA | 0.02 | 0.83 | 0.84 |
| Psychological measures | | | | |
| Right sagittal stratum | | | | |
| PCL | FA | 0.02 | −0.60 | 0.75 |
| PCL | RD | 0.04 | 0.66 | 0.67 |
| CES-D | FA | 0.03 | −0.61 | 0.75 |
| CES-D | RD | 0.03 | 0.69 | 0.74 |
| Left insular | | | | |
| PCS | MD | 0.03 | 0.68 | 0.70 |
| Left Corticospinal tract | | | | |
| PCS | AD | 0.04 | 0.69 | 0.64 |
| Left superior longitudinal fasciculus | | | | |
| PCL | MD | 0.03 | 0.73 | 0.71 |
| PCL | RD | 0.03 | 0.77 | 0.71 |
| CES-D | MD | 0.03 | 0.85 | 0.73 |
| CES-D | RD | 0.04 | 0.78 | 0.72 |
| Clinical measures | | | | |
| Left Corticospinal tract | | | | |
| MPQ | RD | 0.01 | 0.67 | 0.84 |

Statistical Model 2 (Equation (2)) was used with age, sex, and the DVRS scores as covariates. Abbreviations: *r* = correlation coefficient; *R*² = coefficient of determination for goodness of fit.

The DTI metrics also predicted later psychological outcomes (Table 2, middle section). PCL and CES-D were predicted by both FA (negative association) and RD (positive association) in the right sagittal stratum with large correlation coefficients ($|r| > 0.60$, $p < 0.05$). They were also predicted by MD and RD in the left superior longitudinal fasciculus (positive association, $r > 0.73$, $p < 0.05$). PCS was predicted by MD in the left insular (positive association, $r = 0.68$, $p = 0.03$) and AD in the left corticospinal tract (positive association, $r = 0.69$, $p = 0.04$).

Regarding the clinical pain measures, the MPQ pain scale at 6 months also increased with elevated RD in the left corticospinal tract ($r = 0.67$, $p = 0.01$) at 1 month post-injury. All above associations had a median goodness-of-fit (R^2) of 0.75 (ranging from 0.64 to 0.94).

3.3. Between Group Prediction Power Differences

The associations between the early DTI metrics and later pain-related measures had significant group differences in three cerebral white-matter tracts, including the left insula, right sagittal stratum, and left superior longitudinal fasciculus (Table 3 and Figures 3A, 4A and 5A). While the mTBI group had significant associations indicating the predictivity of the early DTI metrics and later pain and psychological outcomes (Table 3), the control group did not have any significant associations ($p_{\text{con}} > 0.05$, Table 3). Overall, PCL and CES-D are the most sensitive psychological measures to early microstructural changes after mTBI. The directionality of the associations can be evaluated by the scatter plots in Figures 3–5, where worse psychological scores in the mTBI group were associated with and could be predicted by elevated diffusivities (MD and RD) and reduced tissue micro-organization (FA).

Table 3. Significant group differences in the associations between the DTI metrics at 1 month post-injury and pain-related measures at 6 months post-injury.

| | | Model 3 | | mTBI (post hoc) | | Control (post hoc) | |
|---------------------------------------|----|------------------|-------|-------------------|-------------------|--------------------|------------------|
| DTI Metrics | | p_{int} | R^2 | p_{mTBI} | r_{mTBI} | p_{con} | r_{con} |
| Quantitative sensory tests (QST) | | | | | | | |
| Left insula | | | | | | | |
| PPT | AD | 0.04 | 0.53 | 0.02 | 0.13 | 0.35 | −0.10 |
| Psychological measures | | | | | | | |
| Right sagittal stratum | | | | | | | |
| PCL | FA | 0.00 * | 0.53 | 0.02 | −0.60 | 0.8 | −0.04 |
| PCL | RD | 0.01 | 0.55 | 0.04 | 0.66 | 0.65 | −0.04 |
| CES-D | FA | 0.01 | 0.48 | 0.03 | −0.61 | 0.19 | 0.14 |
| CES-D | RD | 0.01 | 0.54 | 0.03 | 0.69 | 0.18 | −0.15 |
| Left superior longitudinal fasciculus | | | | | | | |
| PCL | MD | 0.03 | 0.52 | 0.03 | 0.73 | 0.27 | −0.26 |
| CES-D | MD | 0.02 | 0.57 | 0.03 | 0.85 | 0.45 | 0.04 |
| CES-D | RD | 0.05 | 0.51 | 0.04 | 0.78 | 0.20 | −0.19 |

Statistical Model 3 (Equation (3)) with group interaction term was used with age, sex, and the DVRS scores as covariates. Post hoc associations using Model 2 (Equation (2)) were performed for individual groups (i.e., the mTBI and control groups). Abbreviations: p_{int} = significance level of the group interaction term in Equation (3); p_{mTBI} = significance level of the association between DTI and pain-related measures for the mTBI group; r_{mTBI} = correlation coefficient for the mTBI group; p_{con} = significance level of the association between DTI and pain-related measures for the control group; r_{con} = correlation coefficient for the control group. Bold numbers indicate statistical significance with $p < 0.05$. * denotes $p_{\text{int}} = 0.0044$.

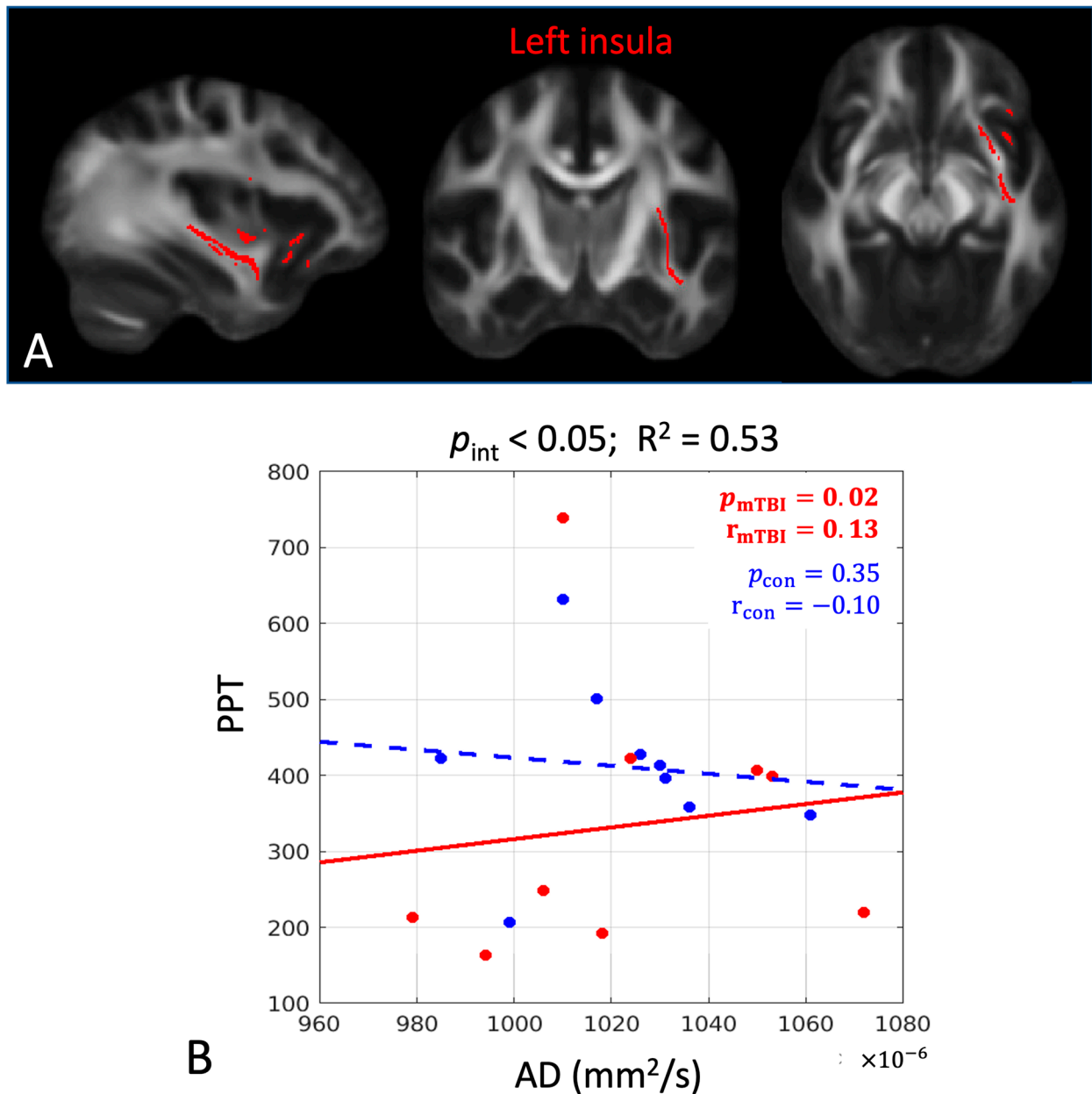


Figure 3. In the left insula, there was a significant group difference in the associations between axial diffusivity (AD) at 1 month post-injury and the pressure pain threshold (PPT) of the trigeminal sensitization at 6 months post-injury. (A) The significant white-matter tract in the left insula is shown in red. (B) Scatter plots with post hoc correlation results. The mTBI group had a significant positive association (red dots and solid line), while the control group did not (blue dots and dashed line). Abbreviations: p_{int} = significance level of the group interaction term in Equation (3); R^2 = overall coefficient of determination for goodness of fit for Model 3; p_{mTBI} = significance level of the association for the mTBI group; r_{mTBI} = correlation coefficient for the mTBI group; p_{con} = significance level of the association for the control group; r_{con} = correlation coefficient for the control group. Bold numbers indicate statistical significance with $p < 0.05$.

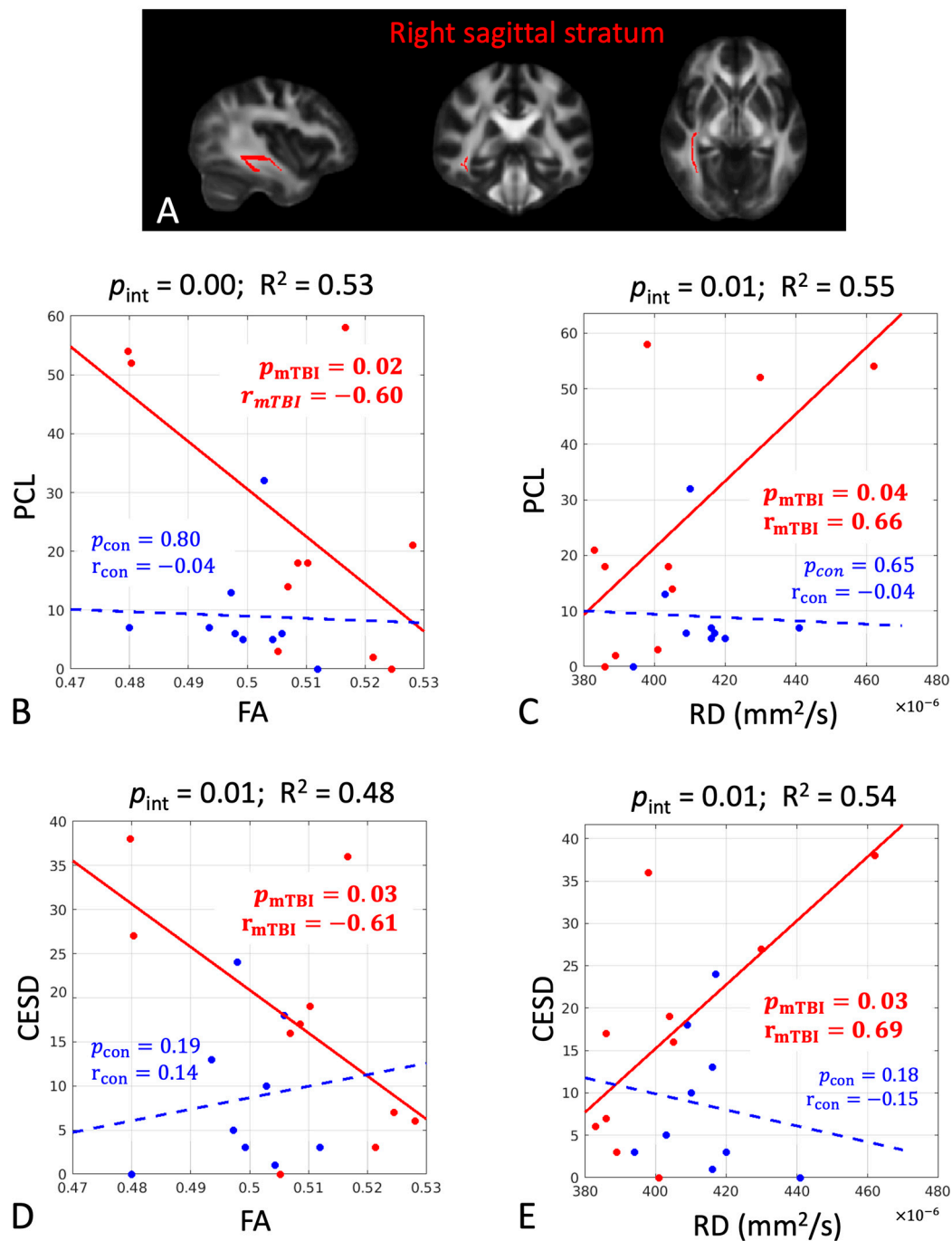


Figure 4. In the right sagittal stratum, there were significant group differences in the associations between the DTI metrics of fractional anisotropy (FA) and radial diffusivity (RD) at 1 month post-injury and the psychological measures of post-traumatic stress symptoms questionnaire score (PCL) and the depression scale at 6 months post-injury (CESD). (A) The significant white-matter tract is shown in red. (B–E) Scatter plots with post hoc correlation results. The mTBI group had a significant positive association (red dots and solid line), while the control group did not (blue dots and dashed line). Abbreviations: p_{int} = significance level of the group interaction term in Equation (3); R^2 = overall coefficient of determination for goodness of fit for Model 3; p_{mTBI} = significance level of the association for the mTBI group; r_{mTBI} = correlation coefficient for the mTBI group; p_{con} = significance level of the association for the control group; r_{con} = correlation coefficient for the control group. Bold numbers indicate statistical significance with $p < 0.05$.

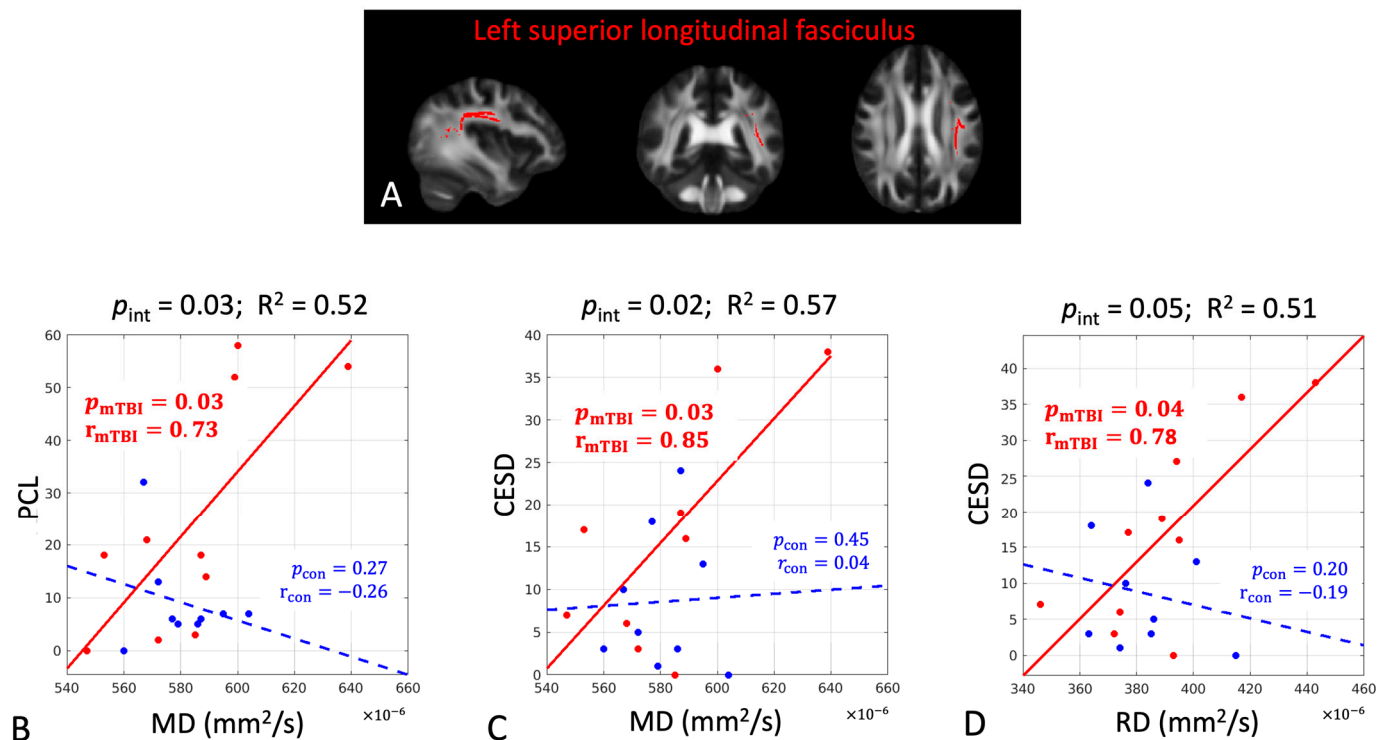


Figure 5. In the left superior longitudinal fasciculus, there were significant group differences in the associations between the DTI metrics of mean diffusivity (MD) and radial diffusivity (RD) at 1 month post-injury and the psychological measures of posttraumatic stress symptoms questionnaire score (PCL) and the depression scale (CESD) at 6 months post-injury. (A) The significant white-matter tract is shown in red. (B–D) Scatter plots with post hoc correlation results. The mTBI group had a significant positive association (red dots and solid line), while the control group did not (blue dots and dashed line). Abbreviations: p_{int} = significance level of the group interaction term in Equation (3); R^2 = overall coefficient of determination for goodness of fit for Model 3; p_{mTBI} = significance level of the association for the mTBI group; r_{mTBI} = correlation coefficient for the mTBI group; p_{con} = significance level of the association for the control group; r_{con} = correlation coefficient for the control group. Bold numbers indicate statistical significance with $p < 0.05$.

4. Discussion

In this study, we performed DTI to detect white-matter microstructural changes in mTBI subjects and their relationships with headache and risk factors for the development of persistent PTH. AD was found to be significantly lower in the forceps major in the subacute phase (1 month) of mTBI. The forceps major connects the prefrontal and fronto-orbital regions, and its impairment may suggest impaired perceptual, cognitive, and motor-related functions following injury [71,72]. Lower AD in the mTBI participants is supported by previous studies [39]. For patients with TBI, the previous literature using automated fiber quantification has also identified subtle reductions in RD in this region [73]. In addition, studies on migraine have found lower AD in forceps minor among migraineurs, as well as in the white-matter fiber bundle connecting the mPFC and amygdala, which is associated with pain chronification [45,46].

Our results suggest that the early DTI metrics were predictive of later pain- and psychological-related measures. For the quantitative sensory tests, decreased white-matter organization predicted increased endogenous facilitation of pain and decreased endogenous inhibition of pain. Additionally, decreased parallel water diffusion (i.e., AD along the axonal orientation) predicted increased pain sensitization of the head area. The early DTI metrics were also sensitive to psychological measures. Decreased white-matter organization was associated with greater post-traumatic stress and depression symptoms. On the

other hand, increased diffusivities were associated with later post-traumatic stress, pain catastrophizing, and depression symptoms. Increased diffusivities were also associated with greater self-reported headaches. The predictivity of the DTI metrics had significant group differences in the psychological measures and PPT, in which the control group did not exhibit such relationships.

The direction of DTI metrics changes may have clinical implications. For example, “an abnormal increase in MD may indicate destruction of the tissue microarchitectures such as axonal beading, cellular swelling, demyelination, or brain edema. An abnormal increase in RD indicates structural destruction perpendicular to the axons such as demyelination, while an abnormal increase in AD indicates structural destruction parallel to the axons such as destruction of cytoskeletons. An abnormal decrease in FA may indicate disorganization axons or demyelination” [44]. In this study, the overall directionalities of the associations to predict worse QST, psychological, and clinical measures at 6 months post-injury were decreased anisotropy (FA) and increased diffusivities (i.e., MD, AD, and RD). Such directionalities may indicate degraded white-matter organizations with dispersed and impaired ordering of axonal fibers and increased intra- and extra-axonal space, enabling freedom of water diffusion. Our results, which demonstrated that higher water mean diffusion is linked to lower clinical outcomes, are consistent with the previous literature. One study showed that mTBI patients with poor clinical tests had elevated MD in the bilateral superior longitudinal fasciculus 4 months after injury [42]. Increased MD in the bilateral cingulum angular bundles were also associated with high headache frequency in persistent PTH patients [47].

From our results, the most sensitive white-matter tracts appeared to be the left insula, right sagittal stratum, and left superior longitudinal fasciculus. Insula is an essential component of the pain matrix for pain perception with extensive structural connections to the prefrontal, parietal, and central cingulate gyri [74–76]. Striatum, composed by caudate, putamen, and ventral striatum, receives afferents from the cortex, midbrain, and thalamus and delivers signal to the basal ganglia [77,78]. The neural activity in striatum is mainly in response to movements and rewards [79,80]. The superior longitudinal fasciculus (SLF), which connects the frontal, parietal, and occipital lobes [39], is highly relevant to prefrontal cortical pain modulation [40,41].

There are several limitations in this study. The primary constraint was the modest sample sizes, which may minimize the capability of detecting small effect sizes, limit generalizability, restrict statistical analyses from performing multiple comparisons, and increase the risk of type II errors [81]. The limitation came from the general challenges in longitudinal recruitment of TBI patients with comprehensive quantitative pain-related measures. Nevertheless, the effect sizes, statistical evaluators independent from sample sizes, of the associations (i.e., r , the correlation coefficients) in Tables 2 and 3 are strong and are larger than 0.6. Meanwhile, our findings are consistent with previous studies that have reported similar group differences in diffusivity or significant associations between diffusion measures and pain metrics [39,42,73]. We believe that with multiple steps of direct association analyses and interaction analyses, our results can still provide the community with useful knowledge and effect sizes for future large-scale study designs. Furthermore, the diffusion tensor assumption has its limitations, as it uses a Gaussian distribution to summarize overall water diffusion behavior within an imaging voxel comprising multiple tissue types, crossing fibers, and diffusion compartments. This approach may not accurately reflect the true complexity of brain tissue. We, therefore, had limited our analyses to the center of the white-matter tracts (skeletonized white-matter ROIs), where the diffusion tensor assumption is less violated. Future diffusion MRI could focus on biophysical modeling, such as neurite orientation dispersion and density imaging [82] or kurtosis-based

white-matter tract integrity imaging [83], to produce more biologically specific diffusion metrics. In summary, while our study provides meaningful inputs to the understanding of association between mTBI and pain in PTH, future research should focus on larger sample sizes, long-term follow-up for studying chronicity and progression of PTH, and more advanced imaging techniques to enhance the robustness and applicability of the findings.

There have been very few longitudinal studies systemically examining the pain-related white-matter changes after mTBI [50]. Here, we investigated the associations between white-matter integrity and the comprehensive measures of pain-related sensory, psychological, and clinical outcomes at the subacute to chronic stage. Using our sophisticated image-processing pipelines and analysis with an interaction model, we demonstrated that the DTI metrics in white-matter are predictive of pain and psychological measures in mTBI. Despite the limitations, this study provides critical insights and effect sizes, paving the way for future studies. One key implication from our study is that pain threshold measurements may be implemented as a standard add-on for mTBI participants to better understand pain-related changes over time. Additionally, given the observed associations between diffusion imaging and pain, psychological, and clinical measures, diffusion imaging could serve as a non-invasive and pain-free method to predict chronic, persistent pain in individuals with mTBI. Lastly, considering all four DTI metrics provides a more comprehensive interpretation of the microstructural mechanisms underpinning mTBI and PTH, providing potential therapeutic targets.

5. Conclusions

Our longitudinal study demonstrated that the DTI metrics at 1 month post-injury are sensitive to mTBI and are predictive of pain and psychological measures in the chronic stage of mTBI at six-months post-injury.

Supplementary Materials: The following supporting information can be downloaded at <https://www.mdpi.com/article/10.3390/diagnostics15050642/s1>: Table S1: Kolmogorov-Smirnov Normality Test: *p*-values for Patient and Control Groups Across QST, Psychological, and Clinical Measures (6 month); Table S2: Kolmogorov-Smirnov Normality Test: *p*-values for Patient and Control Groups Across DTI metrics.

Author Contributions: Conceptualization, F.A.W., K.M.N., and Y.-C.W.; methodology, F.A.W., K.M.N., and Y.-C.W.; formal analysis, H.-C.Y.; investigation, H.-C.Y., F.A.W., K.M.N., and Y.-C.W.; data curation, H.-C.Y. and T.N.; writing—original draft preparation, H.-C.Y.; writing—review and editing, T.N., F.A.W., K.M.N., and Y.-C.W.; visualization, H.-C.Y.; supervision, F.A.W., K.M.N., and Y.-C.W.; project administration, F.A.W., K.M.N., and Y.-C.W.; funding acquisition, F.A.W., K.M.N., and Y.-C.W. All authors have read and agreed to the published version of the manuscript.

Funding: This study is supported by funding from the Indiana Clinical and Translational Sciences Institute (UM1TR004402), which is funded in part by UL1TR002529 (FAW KMN YCW), U.S. Army Medical Research and Development Command (W81XWH-18-1-0433 and W81XWH-18-1-0434 to FAW and KMN) and National Institutes of Health (R01 NS102415 to FAW and R01 NS112303 to YCW).

Institutional Review Board Statement: The study was conducted in accordance with the Declaration of Helsinki and approved by the Indiana University Human Subjects and Institutional Review Board of Indiana University School of Medicine (protocol code 1804170492 and 9 July 2018).

Informed Consent Statement: All participants reviewed and signed a written informed-consent form approved by the Indiana University Institutional review board.

Data Availability Statement: De-identified data from this study will be made publicly available in (FITBIR). Analytic code used to conduct the analyses will be made available in (GITHUB).

Acknowledgments: Data presented herein were obtained at the Department of Radiology and Imaging Sciences at the Indiana University School of Medicine. We gratefully acknowledge the excellent technical assistance of Paul Territo and Scott Persohn. The authors wish to also thank the individuals who participated in this research study, without whom this research would not be possible.

Conflicts of Interest: All authors read and approved the final manuscript. The authors declare no conflicts of interest. The funders had no role in the design of the study; in the collection, analyses, or interpretation of data; in the writing of the manuscript; or in the decision to publish the results. The submitted work has not been published previously and is not being considered for publication elsewhere. Material has not been reproduced from prior publications, whether by the same or different authors. Any previously published material is explicitly quoted and referenced. Each author has read and completed all sections of the Author Disclosure Form. I verify that appropriate Institutional Review Board (IRB) and/or ethics committee approval has been obtained for the use of human subjects. I verify that written informed consent was obtained from all research participants.

Abbreviations

The following abbreviations are used in this manuscript:

| | |
|----------|---|
| DTI | Diffusion tensor imaging |
| mTBI | Mild traumatic brain injury |
| PTH | Post-traumatic headache |
| PPT | Pressure pain thresholds |
| CPM | Conditioned pain modulation |
| MRI | Magnetic resonance imaging |
| SWI | Susceptibility-weighted imaging |
| FA | Fractional anisotropy |
| MD | Mean diffusivity |
| RD | Radial diffusivity |
| AD | Axial diffusivity |
| MMSE | Mini Mental Status Examination |
| QST | Quantitative sensory tests |
| TS | Temporal summation |
| CPM | Conditioned pain modulation |
| HA | Headache intensity |
| MPQ | McGill Pain Questionnaire |
| PRI | Pain rating index |
| DVPRS | Defense and Veterans Pain Rating Scale |
| TBI-QOL | TBI Quality of Life |
| PTSD | Post-Traumatic Stress Disorder |
| PCS | Pain Catastrophizing Scale |
| CES-D | Center for Epidemiological Studies-Depression Scale |
| IRSPGR | Inversion recovery-prepared spoiled gradient-echo |
| GRE | Gradient-echo sequence |
| FSL | FMRIB Software Library |
| MNI | Montreal Neurological Institute |
| ROIs | Regions-of-interest |
| TBBS | Tract-based spatial statistics |
| <i>p</i> | Significance level |
| JHU | Johns Hopkins University |
| mo | Month |
| PCL | Post-traumatic stress symptoms questionnaire |
| <i>r</i> | Correlation coefficient |

| | |
|------------|---|
| R^2 | Coefficient of determination for goodness of fit |
| p_{int} | Significance level of the group interaction term |
| p_{mTBI} | Significance level of the association between DTI and pain-related measures for the mTBI group |
| r_{mTBI} | Correlation coefficient for the mTBI group |
| p_{con} | Significance level of the association between DTI and pain-related measures for the control group |
| r_{con} | Correlation coefficient for the control group |
| SLF | Superior longitudinal fasciculus |

References

1. Nampiaparampil, D.E. Prevalence of chronic pain after traumatic brain injury: A systematic review. *JAMA* **2008**, *300*, 711–719. [[CrossRef](#)] [[PubMed](#)]
2. Lucas, S.; Hoffman, J.M.; Bell, K.R.; Dikmen, S. A prospective study of prevalence and characterization of headache following mild traumatic brain injury. *Cephalalgia* **2014**, *34*, 93–102. [[CrossRef](#)] [[PubMed](#)]
3. Hoffman, J.M.; Lucas, S.; Dikmen, S.; Temkin, N. Clinical perspectives on headache after traumatic brain injury. *PMR* **2020**, *12*, 967–974. [[CrossRef](#)]
4. Zhang, Y.; Kong, Q.; Chen, J.; Li, L.; Wang, D.; Zhou, J. International Classification of Headache Disorders 3rd edition beta-based field testing of vestibular migraine in China: Demographic, clinical characteristics, audiometric findings and diagnosis statuses. *Cephalalgia* **2016**, *36*, 240–248. [[CrossRef](#)]
5. Channell, M.K.; Mueller, L.L.; Hahn, R. Management of chronic posttraumatic headache: A multidisciplinary approach. *J. Osteopath. Med.* **2009**, *109*, 509–513.
6. Defrin, R. Chronic post-traumatic headache: Clinical findings and possible mechanisms. *J. Man. Manip. Ther.* **2014**, *22*, 36–43. [[CrossRef](#)]
7. Rasmussen, B.K.; Olesen, J. Symptomatic and nonsymptomatic headaches in a general population. *Neurology* **1992**, *42*, 1225. [[CrossRef](#)]
8. Ashina, H.; Iljazi, A.; Al-Khazali, H.M.; Ashina, S.; Jensen, R.H.; Amin, F.M.; Ashina, M.; Schytz, H.W. Persistent post-traumatic headache attributed to mild traumatic brain injury: Deep phenotyping and treatment patterns. *Cephalalgia* **2020**, *40*, 554–564. [[CrossRef](#)]
9. Naugle, K.M.; Carey, C.; Evans, E.; Saxe, J.; Overman, R.; White, F.A. The role of deficient pain modulatory systems in the development of persistent post-traumatic headaches following mild traumatic brain injury: An exploratory longitudinal study. *J. Headache Pain* **2020**, *21*, 138. [[CrossRef](#)]
10. Sahbaie, P.; Tajerian, M.; Yang, P.; Irvine, K.A.; Huang, T.-T.; Luo, J.; Wyss-Coray, T.; Clark, J.D. Nociceptive and cognitive changes in a murine model of polytrauma. *J. Pain* **2018**, *19*, 1392–1405. [[CrossRef](#)]
11. Schwedt, T.J.; Chong, C.D.; Peplinski, J.; Ross, K.; Berisha, V. Persistent post-traumatic headache vs. migraine: An MRI study demonstrating differences in brain structure. *J. Headache Pain.* **2017**, *18*, 87. [[CrossRef](#)] [[PubMed](#)]
12. Farkas, O.; Povlishock, J.T. Cellular and subcellular change evoked by diffuse traumatic brain injury: A complex web of change extending far beyond focal damage. *Prog. Brain Res.* **2007**, *161*, 43–59. [[CrossRef](#)] [[PubMed](#)]
13. Büki, A.; Povlishock, J. All roads lead to disconnection?—Traumatic axonal injury revisited. *Acta Neurochir.* **2006**, *148*, 181–194. [[CrossRef](#)]
14. Dikranian, K.; Cohen, R.; Mac Donald, C.; Pan, Y.; Brakefield, D.; Bayly, P.; Parsadanian, A. Mild traumatic brain injury to the infant mouse causes robust white matter axonal degeneration which precedes apoptotic death of cortical and thalamic neurons. *Exp. Neurol.* **2008**, *211*, 551–560. [[CrossRef](#)] [[PubMed](#)]
15. Oppenheimer, D.R. Microscopic lesions in the brain following head injury. *J. Neurol. Neurosurg. Psychiatry* **1968**, *31*, 299. [[CrossRef](#)]
16. Blumbergs, P.; Scott, G.; Manavis, J.; Wainwright, H.; Simpson, D.; McLean, A. Staining of amyloid precursor protein to study axonal damage in mild head injury. *Lancet* **1994**, *344*, 1055–1056. [[CrossRef](#)]
17. Bigler, E.D. Neuropsychological results and neuropathological findings at autopsy in a case of mild traumatic brain injury. *J. Int. Neuropsychol. Soc.* **2004**, *10*, 794–806. [[CrossRef](#)]
18. McKee, A.C.; Stein, T.D.; Nowinski, C.J.; Stern, R.A.; Daneshvar, D.H.; Alvarez, V.E.; Lee, H.-S.; Hall, G.; Wojtowicz, S.M.; Baugh, C.M. The spectrum of disease in chronic traumatic encephalopathy. *Brain* **2013**, *136*, 43–64. [[CrossRef](#)]
19. Koerte, I.K.; Hufschmidt, J.; Muehlmann, M.; Lin, A.P.; Shenton, M.E. Advanced neuroimaging of mild traumatic brain injury. In *Translational Research in Traumatic Brain Injury*; CRC Press: Boca Raton, FL, USA, 2016.
20. Ofoghi, Z.; Dewey, D.; Barlow, K.M. A systematic review of structural and functional imaging correlates of headache or pain after mild traumatic brain injury. *J. Neurotrauma* **2020**, *37*, 907–923. [[CrossRef](#)]

21. Baliki, M.N.; Petre, B.; Torbey, S.; Herrmann, K.M.; Huang, L.; Schnitzer, T.J.; Fields, H.L.; Apkarian, A.V. Corticostriatal functional connectivity predicts transition to chronic back pain. *Nat. Neurosci.* **2012**, *15*, 1117–1119. [\[CrossRef\]](#)
22. Vachon-Preseu, E.; Tetreault, P.; Petre, B.; Huang, L.; Berger, S.E.; Torbey, S.; Baria, A.T.; Mansour, A.R.; Hashmi, J.A.; Griffith, J.W. Corticolimbic anatomical characteristics predetermine risk for chronic pain. *Brain* **2016**, *139*, 1958–1970. [\[CrossRef\]](#) [\[PubMed\]](#)
23. Hashmi, J.A.; Baliki, M.N.; Huang, L.; Baria, A.T.; Torbey, S.; Hermann, K.M.; Schnitzer, T.J.; Apkarian, A.V. Shape shifting pain: Chronification of back pain shifts brain representation from nociceptive to emotional circuits. *Brain* **2013**, *136*, 2751–2768. [\[CrossRef\]](#) [\[PubMed\]](#)
24. Yu, R.; Gollub, R.L.; Spaeth, R.; Napadow, V.; Wasan, A.; Kong, J. Disrupted functional connectivity of the periaqueductal gray in chronic low back pain. *NeuroImage Clin.* **2014**, *6*, 100–108. [\[CrossRef\]](#) [\[PubMed\]](#)
25. Georgopoulos, V.; Akin-Akinyosoye, K.; Zhang, W.; McWilliams, D.F.; Hendrick, P.; Walsh, D.A. Quantitative sensory testing and predicting outcomes for musculoskeletal pain, disability, and negative affect: A systematic review and meta-analysis. *Pain* **2019**, *160*, 1920–1932. [\[CrossRef\]](#)
26. Amyot, F.; Arciniegas, D.B.; Brazaitis, M.P.; Curley, K.C.; Diaz-Arrastia, R.; Gandjbakhche, A.; Herscovitch, P.; Hinds, S.R.; Manley, G.T.; Pacifico, A. A review of the effectiveness of neuroimaging modalities for the detection of traumatic brain injury. *J. Neurotrauma* **2015**, *32*, 1693–1721. [\[CrossRef\]](#)
27. Haller, S.; Haacke, E.M.; Thurnher, M.M.; Barkhof, F. Susceptibility-weighted imaging: Technical essentials and clinical neurologic applications. *Radiology* **2021**, *299*, 3–26. [\[CrossRef\]](#)
28. Stephens, J.A.; Liu, P.; Lu, H.; Suskauer, S.J. Cerebral blood flow after mild traumatic brain injury: Associations between symptoms and post-injury perfusion. *J. Neurotrauma* **2018**, *35*, 241–248. [\[CrossRef\]](#)
29. Wang, Y.; Bartels, H.M.; Nelson, L.D. A systematic review of ASL perfusion MRI in mild TBI. *Neuropsychol. Rev.* **2023**, *33*, 160–191. [\[CrossRef\]](#)
30. Li, F.; Zhang, D.; Ren, J.; Xing, C.; Hu, L.; Miao, Z.; Lu, L.; Wu, X. Connectivity of the insular subdivisions differentiates posttraumatic headache-associated from nonheadache-associated mild traumatic brain injury: An arterial spin labelling study. *J. Headache Pain* **2024**, *25*, 103. [\[CrossRef\]](#)
31. Fan, F.; Beare, R.; Takagi, M.; Anderson, N.; Bressan, S.; Clarke, C.J.; Davis, G.A.; Dunne, K.; Fabiano, F.; Hearps, S.J.C.; et al. Cerebral blood flow in children with persisting postconcussive symptoms and posttraumatic headache at 2 weeks postconcussion. *J. Neurosurg. Pediatr.* **2023**, *32*, 1–8. [\[CrossRef\]](#)
32. Belanger, H.G.; Vanderploeg, R.D.; Curtiss, G.; Warden, D.L. Recent neuroimaging techniques in mild traumatic brain injury. *J. Neuropsychiatry Clin. Neurosci.* **2007**, *19*, 5–20. [\[CrossRef\]](#)
33. Bigler, E.D.; Bazarian, J.J. Diffusion tensor imaging: A biomarker for mild traumatic brain injury? *Neurology* **2010**, *74*, 626–627. [\[CrossRef\]](#)
34. Lipton, M.L.; Kim, N.; Park, Y.K.; Hulkower, M.B.; Gardin, T.M.; Shifteh, K.; Kim, M.; Zimmerman, M.E.; Lipton, R.B.; Branch, C.A. Robust detection of traumatic axonal injury in individual mild traumatic brain injury patients: Intersubject variation, change over time and bidirectional changes in anisotropy. *Brain Imaging Behav.* **2012**, *6*, 329–342. [\[CrossRef\]](#) [\[PubMed\]](#)
35. Gardner, A.; Kay-Lambkin, F.; Stanwell, P.; Donnelly, J.; Williams, W.H.; Hiles, A.; Schofield, P.; Levi, C.; Jones, D.K. A systematic review of diffusion tensor imaging findings in sports-related concussion. *J. Neurotrauma* **2012**, *29*, 2521–2538. [\[CrossRef\]](#)
36. Eierud, C.; Craddock, R.C.; Fletcher, S.; Aulakh, M.; King-Casas, B.; Kuehl, D.; LaConte, S.M. Neuroimaging after mild traumatic brain injury: Review and meta-analysis. *NeuroImage Clin.* **2014**, *4*, 283–294. [\[CrossRef\]](#) [\[PubMed\]](#)
37. Dodd, A.B.; Epstein, K.; Ling, J.M.; Mayer, A.R. Diffusion tensor imaging findings in semi-acute mild traumatic brain injury. *J. Neurotrauma* **2014**, *31*, 1235–1248. [\[CrossRef\]](#) [\[PubMed\]](#)
38. Yuh, E.L.; Cooper, S.R.; Mukherjee, P.; Yue, J.K.; Lingsma, H.F.; Gordon, W.A.; Valadka, A.B.; Okonkwo, D.O.; Schnyer, D.M.; Vassar, M.J. Diffusion tensor imaging for outcome prediction in mild traumatic brain injury: A TRACK-TBI study. *J. Neurotrauma* **2014**, *31*, 1457–1477. [\[CrossRef\]](#)
39. Leung, A.; Yang, E.; Lim, M.; Metzger-Smith, V.; Theilmann, R.; Song, D.; Lin, L.; Tsai, A.; Lee, R. Pain-related white matter tract abnormalities in mild traumatic brain injury patients with persistent headache. *Mol. Pain.* **2018**, *14*, 1744806918810297. [\[CrossRef\]](#)
40. Farmer, M.A.; Huang, L.; Martucci, K.; Yang, C.C.; Maravilla, K.R.; Harris, R.E.; Clauw, D.J.; Mackey, S.; Ellingson, B.M.; Mayer, E.A. Brain white matter abnormalities in female interstitial cystitis/bladder pain syndrome: A MAPP network neuroimaging study. *J. Urol.* **2015**, *194*, 118–126. [\[CrossRef\]](#)
41. Huang, L.; Kutch, J.J.; Ellingson, B.M.; Martucci, K.T.; Harris, R.E.; Clauw, D.J.; Mackey, S.; Mayer, E.A.; Schaeffer, A.J.; Apkarian, A.V. Brain white matter changes associated with urological chronic pelvic pain syndrome: Multisite neuroimaging from a MAPP case-control study. *Pain* **2016**, *157*, 2782–2791. [\[CrossRef\]](#)
42. Messé, A.; Caplain, S.; Paradot, G.; Garrigue, D.; Mineo, J.F.; Soto Ares, G.; Ducreux, D.; Vignaud, F.; Rozec, G.; Desal, H. Diffusion tensor imaging and white matter lesions at the subacute stage in mild traumatic brain injury with persistent neurobehavioral impairment. *Hum. Brain Mapp.* **2011**, *32*, 999–1011. [\[CrossRef\]](#)

43. Kraus, M.F.; Susmaras, T.; Caughlin, B.P.; Walker, C.J.; Sweeney, J.A.; Little, D.M. White matter integrity and cognition in chronic traumatic brain injury: A diffusion tensor imaging study. *Brain* **2007**, *130*, 2508–2519. [\[CrossRef\]](#)
44. Wu, Y.-C.; Harezlak, J.; Elsaid, N.M.; Lin, Z.; Wen, Q.; Mustafi, S.M.; Riggan, L.D.; Koch, K.M.; Nencka, A.S.; Meier, T.B. Longitudinal white-matter abnormalities in sports-related concussion: A diffusion MRI study. *Neurology* **2020**, *95*, e781–e792. [\[CrossRef\]](#)
45. Liu, J.; Mu, J.; Chen, T.; Zhang, M.; Tian, J. White matter tract microstructure of the mPFC-amygdala predicts interindividual differences in placebo response related to treatment in migraine patients. *Hum. Brain Mapp.* **2019**, *40*, 284–292. [\[CrossRef\]](#) [\[PubMed\]](#)
46. Petrušić, I.; Daković, M.; Kačar, K.; Mičić, O.; Zidverc-Trajković, J. Migraine with aura and white matter tract changes. *Acta Neurol. Belg.* **2018**, *118*, 485–491. [\[CrossRef\]](#) [\[PubMed\]](#)
47. Chong, C.D.; Peplinski, J.; Berisha, V.; Ross, K.; Schwedt, T.J. Differences in fibertract profiles between patients with migraine and those with persistent post-traumatic headache. *Cephalalgia* **2019**, *39*, 1121–1133. [\[CrossRef\]](#) [\[PubMed\]](#)
48. Alhilali, L.; Delic, J.; Fakhra, S. Differences in callosal and forniceal diffusion between patients with and without postconcussive migraine. *Am. J. Neuroradiol.* **2017**, *38*, 691–695. [\[CrossRef\]](#)
49. Ghodadra, A.; Alhilali, L.; Fakhra, S. Principal component analysis of diffusion tensor images to determine white matter injury patterns underlying postconcussive headache. *Am. J. Neuroradiol.* **2016**, *37*, 274–278. [\[CrossRef\]](#)
50. Branco, P.; Bosak, N.; Bielefeld, J.; Cong, O.; Granovsky, Y.; Kahn, I.; Yarnitsky, D.; Apkarian, A.V. Structural brain connectivity predicts early acute pain after mild traumatic brain injury. *Pain* **2023**, *164*, 1312–1320. [\[CrossRef\]](#)
51. Mthi, C. Methodological issues and research recommendations for mild traumatic brain injury: The WHO Collaborating Centre Task Force on Mild Traumatic Brain Injury. *J. Rehabil. Med.* **2004**, *43* (Suppl. S43), 113–125. [\[CrossRef\]](#)
52. Naugle, K.M.; Nguyen, T.; Smith, J.A.; Saxe, J.; White, F.A. Racial differences in head pain and other pain-related outcomes after mild traumatic brain injury. *J. Neurotrauma* **2023**, *40*, 1671–1683. [\[CrossRef\]](#)
53. Woolf, C.J. Central sensitization: Implications for the diagnosis and treatment of pain. *Pain* **2011**, *152*, S2–S15. [\[CrossRef\]](#)
54. Filatova, E.; Latysheva, N.; Kurenkov, A. Evidence of persistent central sensitization in chronic headaches: A multi-method study. *J. Headache Pain* **2008**, *9*, 295–300. [\[CrossRef\]](#) [\[PubMed\]](#)
55. Yarnitsky, D. Conditioned pain modulation (the diffuse noxious inhibitory control-like effect): Its relevance for acute and chronic pain states. *Curr. Opin. Anesthesiol.* **2010**, *23*, 611–615. [\[CrossRef\]](#)
56. Yarnitsky, D.; Bouhassira, D.; Drewes, A.; Fillingim, R.; Granot, M.; Hansson, P.; Landau, R.; Marchand, S.; Matre, D.; Nilsen, K. Recommendations on practice of conditioned pain modulation (CPM) testing. *Eur. J. Pain* **2015**, *19*, 805–806. [\[CrossRef\]](#)
57. Melzack, R. The McGill Pain Questionnaire: Major properties and scoring methods. *Pain* **1975**, *1*, 277–299. [\[CrossRef\]](#) [\[PubMed\]](#)
58. Cook, K.F.; Kallen, M.A.; Buckenmaier III, C.; Flynn, D.M.; Hanling, S.R.; Collins, T.S.; Joltes, K.; Kwon, K.; Medina-Torne, S.; Nahavandi, P. Evaluation of the validity and response burden of patient self-report measures of the Pain Assessment Screening Tool and Outcomes Registry (PASTOR). *Mil. Med.* **2017**, *182*, e1851–e1861. [\[CrossRef\]](#) [\[PubMed\]](#)
59. Tulskey, D.S.; Kisala, P.A.; Victorson, D.; Carlozzi, N.; Bushnik, T.; Sherer, M.; Choi, S.W.; Heinemann, A.W.; Chiaravalloti, N.; Sander, A.M. TBI-QOL: Development and calibration of item banks to measure patient reported outcomes following traumatic brain injury. *J. Head Trauma Rehabil.* **2016**, *31*, 40–51. [\[CrossRef\]](#)
60. Weathers, F.W.; Litz, B.T.; Keane, T.M.; Herman, D.S.; Steinberg, H.R.; Huska, J.A.; Kraemer, H.C. The utility of the SCL-90-R for the diagnosis of war-zone related posttraumatic stress disorder. *J. Trauma. Stress* **1996**, *9*, 111–128.
61. Sullivan, M.J.; Bishop, S.R.; Pivik, J. The pain catastrophizing scale: Development and validation. *Psychol. Assess.* **1995**, *7*, 524. [\[CrossRef\]](#)
62. Eaton, W.W.; Muntaner, C.; Smith, C.; Tien, A.; Ybarra, M. Center for epidemiologic studies depression scale: Review and revision. In *The Use of Psychological Testing for Treatment Planning and Outcomes Assessment*; Maruish, M., Ed.; Lawrence Erlbaum: Mahwah, NJ, USA, 2004; pp. 363–377.
63. Veraart, J.; Novikov, D.S.; Christiaens, D.; Ades-Aron, B.; Sijbers, J.; Fieremans, E. Denoising of diffusion MRI using random matrix theory. *Neuroimage* **2016**, *142*, 394–406. [\[CrossRef\]](#) [\[PubMed\]](#)
64. Kellner, E.; Dhital, B.; Kiselev, V.G.; Reiser, M. Gibbs-ringing artifact removal based on local subvoxel-shifts. *Magn. Reson. Med.* **2016**, *76*, 1574–1581. [\[CrossRef\]](#)
65. Jenkinson, M.; Beckmann, C.F.; Behrens, T.E.; Woolrich, M.W.; Smith, S.M. Fsl. *Neuroimage* **2012**, *62*, 782–790. [\[CrossRef\]](#)
66. Tournier, J.-D.; Smith, R.; Raffelt, D.; Tabbara, R.; Dhollander, T.; Pietsch, M.; Christiaens, D.; Jeurissen, B.; Yeh, C.-H.; Connelly, A. MRtrix3: A fast, flexible and open software framework for medical image processing and visualisation. *Neuroimage* **2019**, *202*, 116137. [\[CrossRef\]](#) [\[PubMed\]](#)
67. Avants, B.B.; Tustison, N.; Song, G. Advanced normalization tools (ANTs). *Insight J.* **2009**, *2*, 1–35. [\[CrossRef\]](#)
68. Smith, S.M.; Jenkinson, M.; Johansen-Berg, H.; Rueckert, D.; Nichols, T.E.; Mackay, C.E.; Watkins, K.E.; Ciccarelli, O.; Cader, M.Z.; Matthews, P.M. Tract-based spatial statistics: Voxelwise analysis of multi-subject diffusion data. *Neuroimage* **2006**, *31*, 1487–1505. [\[CrossRef\]](#)

69. Gomez-Beldarrain, M.; Oroz, I.; Zapiain, B.G.; Ruanova, B.F.; Fernandez, Y.G.; Cabrera, A.; Anton-Ladislao, A.; Aguirre-Larracoechea, U.; Garcia-Monco, J.C. Right fronto-insular white matter tracts link cognitive reserve and pain in migraine patients. *J. Headache Pain* **2016**, *17*, 1–12. [\[CrossRef\]](#)
70. Althouse, A.D. Adjust for multiple comparisons? It's not that simple. *Ann. Thorac. Surg.* **2016**, *101*, 1644–1645. [\[CrossRef\]](#)
71. Navas-Sánchez, F.J.; Alemán-Gómez, Y.; Sánchez-Gonzalez, J.; Guzmán-De-Villoria, J.A.; Franco, C.; Robles, O.; Arango, C.; Desco, M. White matter microstructure correlates of mathematical giftedness and intelligence quotient. *Hum. Brain Mapp.* **2014**, *35*, 2619–2631. [\[CrossRef\]](#)
72. Weber, B.; Koschutnig, K.; Schwerdtfeger, A.; Rominger, C.; Papousek, I.; Weiss, E.M.; Tilp, M.; Fink, A. Learning unicycling evokes manifold changes in gray and white matter networks related to motor and cognitive functions. *Sci. Rep.* **2019**, *9*, 4324. [\[CrossRef\]](#)
73. Kang, X.; Coetzee, J.P.; Main, K.L.; Seenivasan, S.; Zhu, K.; Adamson, M.M. Fiber tract integrity in patients with brain injury and chronic health symptoms. *Neuroimage Rep.* **2021**, *1*, 100047. [\[CrossRef\]](#)
74. Segerdahl, A.R.; Mezue, M.; Okell, T.W.; Farrar, J.T.; Tracey, I. The dorsal posterior insula subserves a fundamental role in human pain. *Nat. Neurosci.* **2015**, *18*, 499–500. [\[CrossRef\]](#)
75. Jensen, K.B.; Regenbogen, C.; Ohse, M.C.; Frasnelli, J.; Freiherr, J.; Lundström, J.N. Brain activations during pain: A neuroimaging meta-analysis of patients with pain and healthy controls. *Pain* **2016**, *157*, 1279–1286. [\[CrossRef\]](#)
76. Lenroot, R.K.; Giedd, J.N. Brain development in children and adolescents: Insights from anatomical magnetic resonance imaging. *Neurosci. Biobehav. Rev.* **2006**, *30*, 718–729. [\[CrossRef\]](#) [\[PubMed\]](#)
77. Hikosaka, O.; Takikawa, Y.; Kawagoe, R. Role of the basal ganglia in the control of purposive saccadic eye movements. *Physiol. Rev.* **2000**, *80*, 953–978. [\[CrossRef\]](#) [\[PubMed\]](#)
78. Haber, S.N. The primate basal ganglia: Parallel and integrative networks. *J. Chem. Neuroanat.* **2003**, *26*, 317–330. [\[CrossRef\]](#)
79. Hollerman, J.R.; Tremblay, L.; Schultz, W. Influence of reward expectation on behavior-related neuronal activity in primate striatum. *J. Neurophysiol.* **1998**, *80*, 947–963. [\[CrossRef\]](#)
80. Hollerman, J.R.; Tremblay, L.; Schultz, W. Involvement of basal ganglia and orbitofrontal cortex in goal-directed behavior. *Prog. Brain Res.* **2000**, *126*, 193–215. [\[CrossRef\]](#)
81. Knudson, D.V.; Lindsey, C. Type I and Type II errors in correlations of various sample sizes. *Compr. Psychol.* **2014**, *3*, 3. [\[CrossRef\]](#)
82. Zhang, H.; Schneider, T.; Wheeler-Kingshott, C.A.; Alexander, D.C. NODDI: Practical in vivo neurite orientation dispersion and density imaging of the human brain. *NeuroImage* **2012**, *61*, 1000–1016. [\[CrossRef\]](#)
83. Benitez, A.; Jensen, J.H.; Falangola, M.F.; Nietert, P.J.; Helpert, J.A. Modeling white matter tract integrity in aging with diffusional kurtosis imaging. *Neurobiol. Aging* **2018**, *70*, 265–275. [\[CrossRef\]](#) [\[PubMed\]](#)

Disclaimer/Publisher's Note: The statements, opinions and data contained in all publications are solely those of the individual author(s) and contributor(s) and not of MDPI and/or the editor(s). MDPI and/or the editor(s) disclaim responsibility for any injury to people or property resulting from any ideas, methods, instructions or products referred to in the content.